A differential role for nitric oxide in two forms of physiological angiogenesis in mouse

James L. Williams, David Cartland, Arif Hussain and Stuart Egginton

Angiogenesis Research Group, Centre for Cardiovascular Sciences, University of Birmingham, Birmingham B15 2TT, UK

NO plays a role in a variety of *in vitro* models of angiogenesis, although confounding effects of NO on non-endothelial tissues make its role during *in vivo* angiogenesis unclear. We therefore examined the effects of NO on two physiological models of angiogenesis in mouse skeletal muscle: (1) administration of prazosin (50 mg l^{-1}) thereby increasing blood flow; and (2) muscle overload from surgical ablation of a functional synergist. These models induce angiogenesis via longitudinal splitting and capillary sprouting, respectively. Administration of N^G-nitro-L-arginine (L-NNA) abolished the increase in capillary to fibre ratio (C:F) in response to prazosin administration, along with the increases in luminal filopodia and large endothelial vacuoles. L-NNA prevented luminal filopodia and vacuolisation in response to extirpation, but had no effect on abluminal sprouting, and little effect on C:F. Comparison of mice lacking endothelial (eNOS$^{-/-}$) and neuronal NO synthase (nNOS$^{-/-}$) showed that longitudinal splitting is eNOS-dependent, and Western blotting demonstrated an increase in eNOS but not inducible NOS (iNOS) expression. These data show that there are two pathways of physiological angiogenesis in skeletal muscle characterised by longitudinal splitting and capillary sprouting, respectively. NO generated by eNOS plays an essential role in splitting but not in sprouting angiogenesis, which has important implications for angiogenic therapies that target NO.

(Resubmitted 29 July 2005; accepted after revision 10 November 2005; first published online 17 November 2005)
Corresponding author S. Egginton: Department of Physiology, The Medical School, The University of Birmingham, Birmingham B15 2TT, UK. Email: s.egginton@bham.ac.uk

Angiogenesis is the postnatal mechanism whereby an existing microvascular network is expanded in response to a changing metabolic and mechanical environment (Hudlicka *et al.* 1992). It is essential for ontogenic growth and physiological tissue remodelling or repair, but its inappropriate presence or absence underlies a wide range of pathologies (Folkman, 1995). The classic accounts of capillary growth by abluminal sprouting (Wagner, 1980) are not universally applicable, as physiological angiogenesis may occur in a number of ways. For example, angiogenesis in the endometrium proceeds via the processes of intussusception and capillary elongation (Rogers & Gargett, 1998). A multitude of factors have been shown to promote capillary growth, including soluble chemical mediators, cell–cell contacts and external mechanical factors (Hudlicka *et al.* 1992), so the presence of different forms of angiogenesis is perhaps to be expected. We have previously shown that two morphologically different forms of physiological angiogenesis exist in skeletal muscle, and can be induced separately in rats: chronic elevation of shear stress induced by administration of a vasodilator, the α1-adrenergic receptor antagonist prazosin, caused angiogenesis via longitudinal capillary splitting; whereas sustained stretch as a result of muscle overload through surgical extirpation of a synergist led to angiogenesis via the more-familiar capillary sprouting (Egginton *et al.* 2001). Hence, the mechanisms of angiogenesis in response to differential mechanical stimuli are dependent upon the physical environment encountered by the endothelial cells (ECs).

These morphologically distinct forms of angiogenesis may be mediated by different signalling pathways. For example, while both models show an increase in vascular endothelial growth factor (VEGF) levels, the time course is different with peak VEGF expression preceding increases in capillary formation in the prazosin model, but lagging capillary formation in the extirpation model (Rivilis *et al.* 2002). Previous studies from our laboratory have examined the modulation of angiogenesis by shear stress and confirmed a role both for shear-induced NO and prostaglandin release, and their subsequent importance to resulting angiogenesis (Hudlicka, 1991).

Current paradigms suggest that NO has permissive up-regulatory influences on VEGF production, and that VEGF requires sustained NO release for angiogenesis (Ziche *et al.* 1997; Fukumura *et al.* 2001). It has been

 DOI: 10.1113/jphysiol.2005.095596

suggested that NO mediates the proliferative effects of VEGF *in vitro* (Morbidelli *et al.* 1996; Shizukuda *et al.* 1999); however, the role of NO as an angiogenic agent is controversial. We think this in part reflects the heterogeneity in the capillary growth process, only some elements of which are NO dependent. To test this hypothesis, we induced angiogenesis *in vivo* by two methods resulting in different phenotypes and investigated the role of NO through pharmacological inhibition of all NO synthase (NOS) isoforms using N^G-nitro-L-arginine (L-NNA), compared with specific genetic knockouts of endothelial (eNOS) and neuronal NOS (nNOS) isoforms. We examined the *in vivo* angiogenic response by histochemistry, immunocytochemistry, Western blotting and electron microscopy, thus providing the first detailed analysis of angiogenesis in mouse muscle. In addition, we have been able to identify those aspects of angiogenesis that may be amenable to NO-based angiotherapy.

Methods

Animals

Male C57/BL10 mice weighing 25 ± 3 g (Charles River) were used for all procedures, except when indicated otherwise. Knockout mice ($eNOS^{-/-}$ and $nNOS^{-/-}$ on a C57/BL10 background) were obtained from Jackson Immunoresearch Laboratories. Animals were housed at 21°C with a 12 h light−12 h dark cycle, and access to food and water *ad libitum*. All work was carried out in accordance with the UK Animals (Scientific Procedures) Act 1986.

Induction of angiogenesis

Unilateral extirpation of the tibialis anterior muscle was performed as previously described in rats (Zhou *et al.* 1998), resulting in hyperplasia and hypertrophy of the extensor digitorum longus (EDL) muscle. Briefly, mice were anaesthetised with 10 ml kg^{-1} hypnorm/hypnovel (NVS, National Veterinary Services Ltd., Stoke-on-Trent, UK) anaesthetic, supplemented with inhalation anaesthetic (0–2% halothane; Fluothane, ICI) as necessary. A topical antibiotic (Duplocillin LA, NVS) and systemic analgesic (2.5 ml kg^{-1} buprenophine, s.c., Temgesic, NVS) were administered peri-operatively. Prazosin (50 mg l^{-1}, gift from Pfizer) was dissolved in tap water and administered to animals *ad libitum* as drinking water. Each mouse received approximately 175 μg day^{-1}, based on the average water consumption (which was monitored throughout the experiment).

Flow and blood pressure

Blood flow and pressure were recorded using previously reported methods (Neylon & Marshall, 1991). Briefly, anaesthesia was induced using ketamine (0.1 mg kg^{-1}, Pharmacia) and xylazine (0.01 mg kg^{-1}, Millpledge Pharmaceuticals). The right carotid artery was cannulated to record arterial blood pressure (ABP); heart rate (HR) was derived from the pressure signal. A perivascular flow probe (Transonic 0.5VB flowprobe with T106 meter, Linton Instrumentation, Norfolk, UK) was then placed on the upper portion of the femoral artery to record blood flow. Core temperature was controlled with a heating plate and monitored with a thermistor (Fluke S2 KLS).

Western blotting

EDL muscles were homogenized on ice, then proteins were extracted with 1% NP-40, 0.5% NaDOC and 0.1% SDS in phosphate buffer with a proteinase inhibitor cocktail (Sigma), and protein levels were assayed (detergent-compatible protein assay, Biorad). Protein extracts from three different mice were then pooled and 50 μg total protein was loaded per gel. Western blots were run on a 7.5% polyacrylamide gel, transferred to a polyvinylidene fluoride (PVDF) membrane, blocked with 5% non-fat milk powder in Tris-buffered saline (TBS)/Tween buffer (20 mM Tris base, 137 mM NaCl, 0.1% Tween 20, pH 7.6) for 1 h at room temperature (22° C) and incubated with primary antibodies (eNOS and iNOS, 1 : 200, Transduction Laboratories, KY, USA) for 1 h at room temperature. Membranes were stripped with 0.1% NaOH solution and re-probed similarly with an actin antibody (T-20, Santa Cruz). Films were scanned and semi-quantitatively analysed normalizing NOS isoforms to actin levels, and expressed as a percentage of control tissue.

NOS inhibition

Pharmacological inhibition of all NOS isoforms was performed by adding N^G-nitro-L-alginine (L-NNA, Sigma) to drinking water at a concentration of 100 mg l^{-1}, either 2 days before surgery or at the same time as administration of prazosin. L-NNA-treated animals were given L-NNA in drinking water for 14 days, with a mean daily intake of 350 μg per mouse, based on the average water consumption (which was monitored throughout the experiment). L-NNA was preferred to N^G-nitro-L-arginine methyl ester (L-NAME) due to the adverse effects of chronic L-NAME administration on mice (Morley & Flood, 1992).

Confocal microscopy

Animals were anaesthetised via halothane inhalation and injected with 200 μl rhodamine-conjugated *Griffonia simplicifolia* lectin-1 (2 mg ml^{-1} I.V.; Vector). Animals were left for 5 min under anaesthesia before being killed by cervical dislocation. EDL muscles were dissected and fixed

in 30% w/v sucrose in PBS for 1 h at 4°C. Sections (200 μm) were cut on a frozen microtome and examined using a Leica DM IRE2 microscope.

Histology

Animals were killed by cervical dislocation, and EDL muscles were dissected and snap-frozen in liquid nitrogen-cooled isopentane. Sections (10 μm) were cut on a cryostat microtome and allowed to air-dry before staining. Capillary staining was performed on cool acetone-fixed sections using rhodamine-conjugated *Griffonia simplicifolia* lectin-1 (Vector) at 20 μg ml^{-1} in PBS for 30 min at room temperature out of direct light. Cell turnover was labelled by proliferating cell nuclear antigen (PCNA) staining performed on 4% phosphate-buffered formalin-fixed sections using an anti-PCNA antibody (Santa Cruz) at 1 : 100 for 1 h at room temperature, followed by a cyanine (CY2)-conjugated donkey anti-rabbit antibody (Jackson Immunoresearch) at 1 : 50 for 1 h at room temperature with 20 μg ml^{-1} lectin to allow costaining of capillaries. Sections were viewed under fluorescent illumination on an Olympus BHF-312 microscope, and images were captured on an Olympus 3020 zoom digital camera. Capillaries and fibres were counted with a 270 μm × 270 μm counting square using an unbiased sampling protocol, taking four random areas across each muscle. Capillary supply to skeletal muscle can be measured as either capillary density (mm^{-2}) or as capillary to fibre ratio (C:F). C:F is less sensitive to inter-animal variability in fibre size (Hudlicka *et al.* 1992) and was therefore used throughout.

Electron microscopy

Animals were killed as above and the extensor hallucius proprius (EHP) muscle dissected, following *in situ* superfusion for primary fixation with 2.5% gluteraldehyde in 0.1 M phosphate buffer (pH 7.4) to maintain muscle dimensions and minimise tissue shrinkage. Tissue was immersed in fresh fixative for 30 min and trimmed to expose the medial portion of the muscle and returned to fresh fixative overnight. The tissue was washed, post-fixed in buffered osmium tetroxide (1 h), dehydrated in an ethanol series and cleared in propylene oxide, then vacuum-embedded in Mollenhauer resin with two blocks per animal. Embedded muscle blocks were selected at random from each animal, trimmed and sectioned at 90 nm and collected upon formvar-coated slotted copper grids. Sections were stained with 30% uranyl acetate in methanol followed by Reynolds lead citrate, using standard protocols for viewing under the transmission electron microscope.

Twenty-five capillaries were selected in a systematic random manner from each animal per treatment group, to assess a number of pro-angiogenic variables that could be directly counted the transmission electrn microscope (TEM), e.g. EC number. Photographs of a further 25 capillaries from each section were taken at magnification of × 10 000–15 000 to perform a stereological assessment of capillary dimensions and structure. A counting grid was overlaid onto each print and standard point and intersect counts for cellular components (Egginton *et al.* 1993) were used to quantify a number of indices of EC activity, expressed as volume density (V_V), surface density (S_V) or surface to volume ratio (S/V) of structural components.

Four mice were used and 15 TEM images (× 4000 magnification) were captured from randomly selected views for each animal. Radial distribution of mitochondria from capillaries was measured stereologically using three annuli of uniform area with the nearest termed 'zone 1' and the furthest 'zone 3' (Egginton & Sidell, 1989). The point counts on mitochondria (P_{mit}) and total points on muscle tissue (P_{tot}) were then used to calculate V_v of mitochondria per zone (P_{mit}/P_{tot}). Mean mitochondrial density was calculated as ΣP_{mit} (zones 1–3)/ΣP_{tot} (zones 1–3).

Statistical analysis

All data are presented as mean ± S.E.M. Statistical significance between groups was performed using factorial ANOVA with *post hoc* comparisons among groups using a 5% significance level.

Results

The effects of NO on capillary supply

Both prazosin administration and extirpation significantly increased C:F at 14 days, with the peak rate of angiogenesis occurring between 3 and 7 days, and only a modest increase between 14 and 28 days. Final values were 32% higher in the extirpated group and 29% higher in the prazosin group ($P < 0.05$ *versus* control values of 1.23 ± 0.06, $n = 3$) (Table 1). Capillary density showed the same response as C:F (control, 761 ± 81 mm^{-2}), but with a greater variance due to inter-animal variability in fibre size. Administration of prazosin increased femoral blood flow by 58% compared to controls at 7 days (0.643 ± 0.020 *versus* control of 0.410 ± 0.025 ml min^{-1}, $P < 0.05$). No change in blood flow was seen after extirpation in either the ipsilateral (0.427 ± 0.015 ml min^{-1}) or contralateral (0.413 ± 0.015 ml min^{-1}) limb. Heart rate (control, 354 ± 32 beats min^{-1}) and blood pressure (control, 93.6 ± 5.7 mmHg) were not changed significantly by prazosin administration or extirpation.

Table 1. Time course of the angiogenic response in mouse hindlimb muscle

Treatment	0 days	3 days	7 days	14 days	28 days
Prazosin	1.23 ± 0.06	1.36 ± 0.05	1.38 ± 0.03	1.53 ± 0.10*	1.59 ± 0.06*
Extirpation	1.23 ± 0.06	1.39 ± 0.04	1.44 ± 0.03*	1.54 ± 0.08*	1.62 ± 0.05*
Contralateral	1.23 ± 0.06	1.28 ± 0.01	1.44 ± 0.10	1.41 ± 0.11	1.37 ± 0.52

Capillary to fibre ratio is shown for control animals and prazosin-treated and extirpated animals, and the contralateral limb of extirpated animals at 3, 7 and 14 days. Mean ± S.E.M. ($n = 4$) *$P < 0.05$ *versus* control.

Treatment with L-NNA abolished the increase in C:F seen in response to prazosin treatment

There were no differences in C:F, average fibre size or animal behaviour between animals treated with L-NNA alone and untreated controls (Fig. 1). Knockout animals showed different responses to prazosin administration with the increase in C:F abolished in the $eNOS^{-/-}$ mice, but maintained in the $nNOS^{-/-}$ animals. Synergist extirpation resulted in a comparable increase in C:F in $eNOS^{-/-}$, $nNOS^{-/-}$ and wild-type mice with or without L-NNA treatment. Inhibition of NO production in all three cases caused a small decrease in the magnitude of the response to extirpation at 14 days, approximately 25% greater than control levels (Fig. 1). Western blotting of muscle extracts from prazosin-treated and extirpated animals showed a significant increase in eNOS expression at both 3 days (prazosin, 3.6-fold increase; extirpation, 2.4-fold increase *versus* control, $P < 0.05$, $n = 3$) and 7 days (prazosin, 4.1-fold increase; extirpation 2.9-fold increase in *versus* control, $P < 0.05$, $n = 3$), whereas no up-regulation of iNOS was seen in either model (Fig. 2). Liver tissue (10 μg protein) from lipopolysaccharide (LPS)-treated animals (gift from K. Glen, University of Birmingham) was used as a positive control for iNOS.

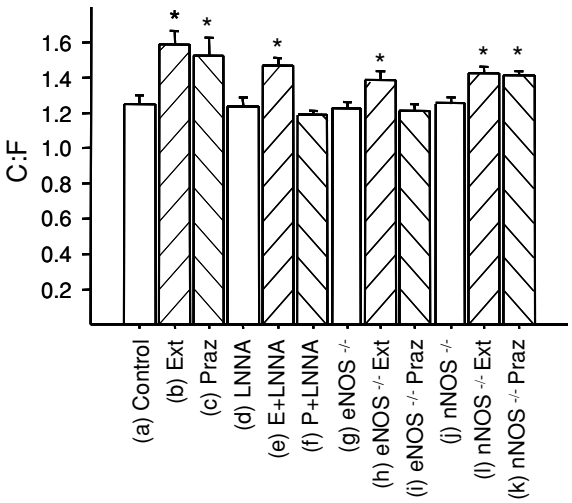

Figure 1. Effects of NO inhibition on angiogenesis
Data are shown for the capillary to fibre ratio (C:F) after 14 days for control, prazosin-treated (praz) and extirpated (ext) wild-type mice, wild-type mice treated with L-NNA (+ LNNA), $eNOS^{-/-}$ mice and $nNOS^{-/-}$ mice. Mean ± S.E.M. *$P < 0.05$ *versus* respective controls.

Ultrastructural responses to NO inhibition in longitudinal splitting

Increased blood flow, and hence probably elevated shear stress, led to a distinct range of responses (Fig. 3) after 7 days. EC number did not increase, indicating a relatively non-proliferative response to the stimuli, confirmed by PCNA staining (Figs 4 and 5). There was a greater prevalence of developed luminal filopodia that protruded mostly from the inter-junctional region of the EC (1.82 ± 0.13 *versus* control of 0.71 ± 0.07 capillary^{-1}, $P < 0.05$) with a complementary increase in S_V, which we interpret to be evidence for the eventual production of a double lumen (Figs 3 and 6) leading to longitudinal splitting of capillaries (Fig. 7). The ECs appeared metabolically active with irregular and thickened surface, increased number of large vacuoles (0.411 ± 0.064 *versus* control of 0.184 ± 0.038, $P < 0.05$ capillary^{-1}) and a decreased luminal area resulting in an increase in both S/V and S_V of the lumen (Fig. 4, Table 2). Mean capillary cross-sectional area was also reduced (5.52 ± 0.27 *versus* control of 7.24 ± 0.33 μm^2, $P < 0.05$), indicative of smaller new capillaries produced by longitudinal splitting (Fig. 4). Capillaries reverted to a control-like ultrastructure upon co-administration of L-NNA with prazosin, with the changes in luminal filopodia, vacuolisation cytoplasmic volume density, lumen S/V and S_V, and capillary area all absent (Fig. 4).

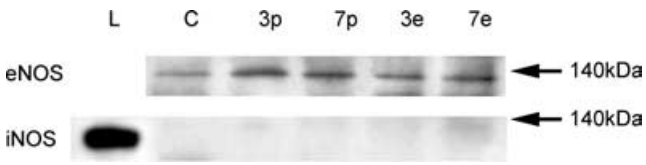

Figure 2. Protein levels of eNOS and iNOS
Protein was extracted from control mice (C), from mice 3 days (3p) and 7 days after prazosin treatment (7p), 3 days (3e) and 7 days after extirpation (7e), and from LPS-treated liver (L; a positive control for iNOS).

Ultrastructural responses to NO inhibition in capillary sprouting

Sustained muscle overload also had specific ultrastructural effects (Fig. 3) at 7 days. There was an increase in EC number (1.84 ± 0.05 *versus* control of 1.47 ± 0.05 capillary^{-1}, $P < 0.05$, Fig. 4) supported by a higher level of capillary-associated PCNA staining (Table 3). The level of endothelial cell abluminal protrusions (0.37 ± 0.05 *versus* control of 0.02 ± 0.01 capillary^{-1}, $P < 0.05$), an early indication of sprouting angiogenesis, also increased, with associated focal loosening of the basement membrane at the sprouting tip (Fig. 4). The endothelium of these enlarged capillaries was active, irregular and thickened (Figs 3 and 6). A role for mural cells was shown by an increase in interstitial PCNA staining alongside increases in pericyte coverage and fibroblast capillary association (Fig. 4; Table 3). A high proportion of abluminal sprouts were seen in physical contact with pericytes ($78.3 \pm 3.86\%$). A novel finding in the mouse was the presence of small luminal filopodia (1.44 ± 0.10 *versus* control of 0.71 ± 0.08 capillary^{-1}, $P < 0.05$) and vacuolisation of the endothelium (0.44 ± 0.06 *versus* control of 0.184 ± 0.04 capillary^{-1}, $P < 0.05$) (Fig. 6). Concurrent administration of L-NNA with extirpation, produced no effects on levels of abluminal sprouts and associated basement membrane breakage (Fig. 4), consistent with C:F remaining high (Fig. 1). Increases in PCNA staining (both capillary-associated and interstitial), EC number, capillary area, pericyte coverage and fibroblast association, and decreases in S_V (lumen, capillary) were unaffected by L-NNA (Figs 4, 5 and 6, and Table 3). However, the modest increase in luminal filopodia, cytoplasmic V_V and vacuolization of capillaries seen in common with prazosin administration were abolished by L-NNA (Fig. 6).

Mitochondrial content

Mitochondrial volume density (V_V) was approximately 20% of the muscle fibre, which increased in response to muscle overload, independent of L-NNA administration. Induced hyperaemia did not invoke a mitochondrial response in the skeletal muscle, and consequently mitochondia, fibre V_V(mit, fib) was unaffected by NO inhibition (Table 4). Mitochondrial density decreased with distance from the capillary and the increase, seen in response to overload occur in regions away from the capillary where the density is lowest (Table 4).

Discussion

Angiogenesis in skeletal muscle may occur via morphologically distinct pathways (Egginton *et al.* 2001), and this study is the first demonstration of two different forms of angiogenesis in the mouse. Despite the apparent similarity to established rat models, inter-species

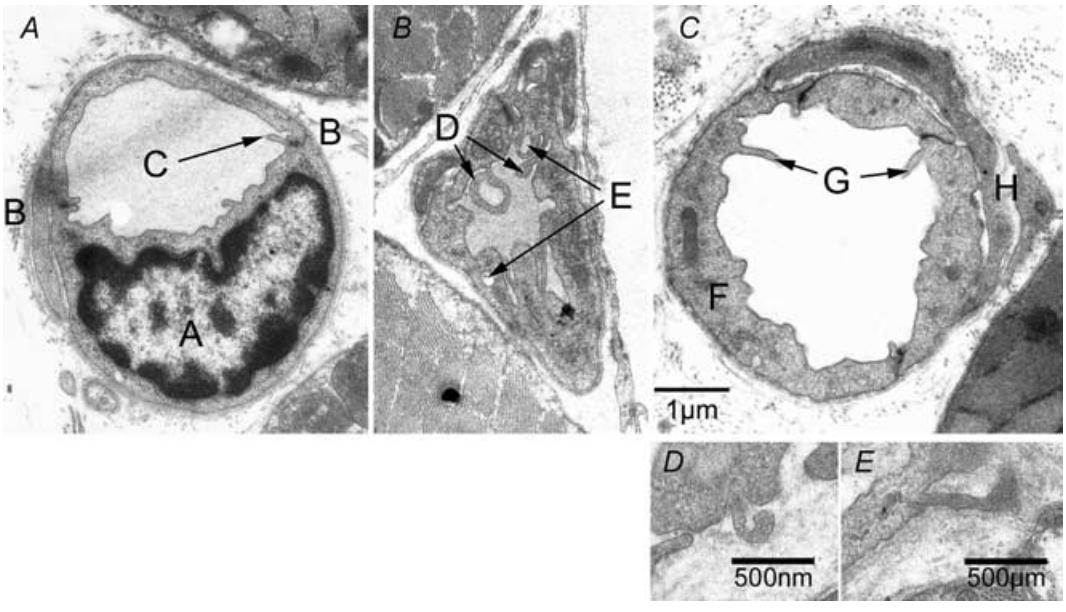

Figure 3. Ultrastructral characterization of the angiogenic response
A, control: capillary showing a thin, uniform endothelium, apart from an endothelial nucleus (N). Two endothelial junctions (J) have a small luminal projection at the junction (F). *B*, prazosin: capillary shows a thickened, highly activated and irregular endothelium with numerous luminal filopodia (F) and vacuoles (V). *C*, extirpation: capillary has three endothelial cells with thickened endothelium (E), small luminal filopodia (F) and extensive pericyte coverage (P). Examples of abluminal sprouts are also shown (*D* and *E*).

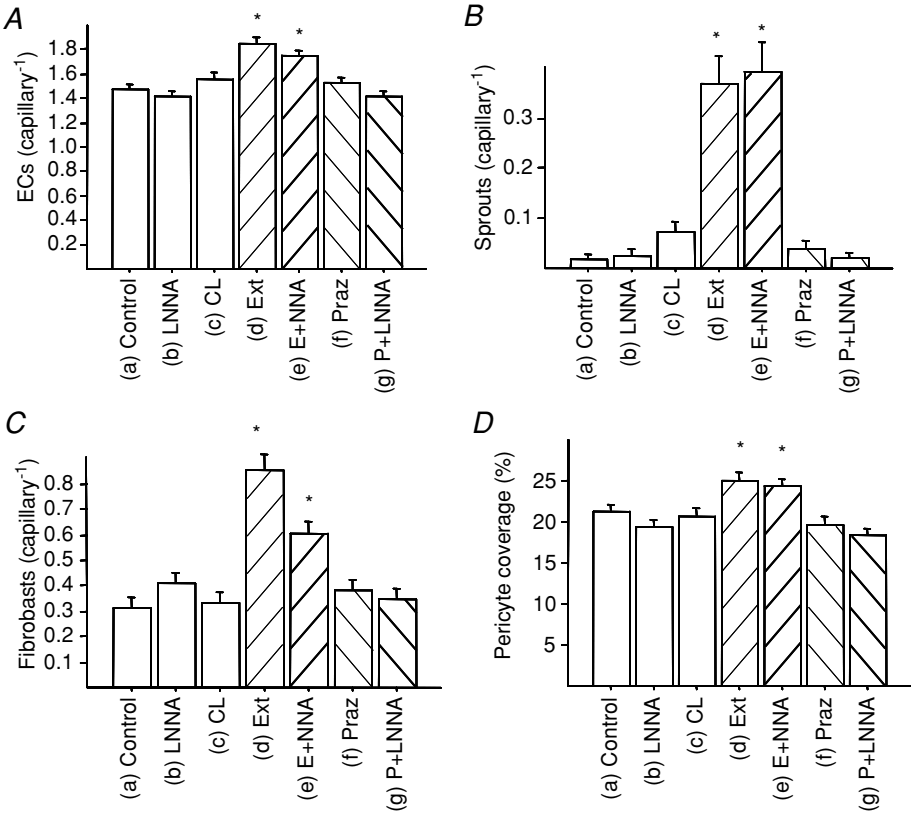

Figure 4. Quantification of major variables in the angiogenic response
A, average number of endothelial cells per capillary cross-section. *B*, average number of abluminal sprouts. *C*, average number of fibroblasts adjacent to a capillary. *D*, percentage of the capillary covered by pericytes. Data are shown for control (a), L-NNA treated (b), extirpated (d), contralateral limb (c), extirpated with L-NNA (e), prazosin treated (f) and prazosin with L-NNA (g). Mean ± S.E.M. ($n = 4$). *$P < 0.05$ *versus* control.

differences may result from, for example, changes in fibre type composition or metabolic scaling effects. Hence, confirmation that the mouse model is comparable to previous data reported for the rat is essential to

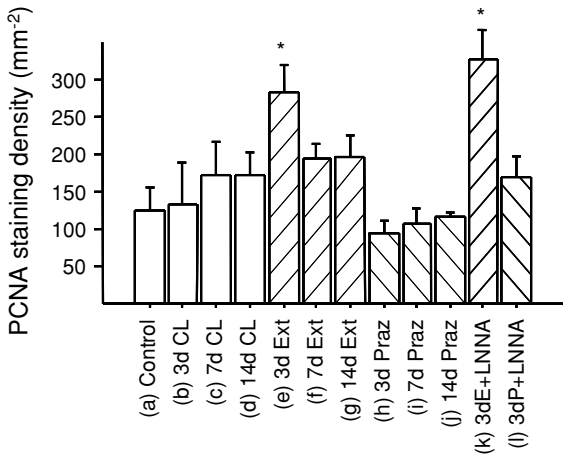

Figure 5. Time course of cell proliferation in mouse EDL
PCNA staining density for control (a), prazosin (b–d), extirpation (e–g) and the contralateral limb (h–j) for 3, 7 and 14 days. Data are also presented for animals that received L-NNA with extirpation (k) and prazosin (l) at 3 days. Mean ± S.E.M. ($n = 4$) *$P < 0.05$ *versus* control.

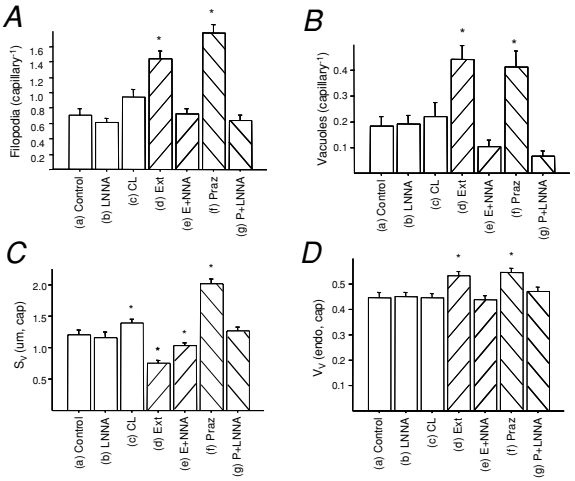

Figure 6. Quantification of major ultrastructural features of the angiogenic response
(A) average number of luminal filopodia per capillary. (B) average number of vacuoles per capillary. (C) surface density and capillary lumen. (D) area density of the cytoplasm as a fraction of the capillary area. Data are shown for control (a), L-NNA treated (b), extirpated (d), contralateral limb (c), extirpated with L-NNA (e), prazosin treated (f) and prazosin with L-NNA (g) D, mean ± S.E.M. ($n = 4$). *$P < 0.05$ *versus* control.

Table 2. Quantification of minor ultrastructural features of the angiogenic response

	Control	L-NNA	Contralateral	Extirpation	E + L-NNA	Prazosin	P + L-NNA
Lumen area (μm^2)	3.3 ± 0.3	3.4 ± 0.4	3.4 ± 0.4	4.2 ± 0.4*	4.4 ± 0.4*	2.2 ± 0.2*	3.2 ± 0.3
V_V (lumen) (%)	43.5 ± 2.4	41.6 ± 3.6	40.2 ± 2.5	33.3 ± 2.1*	38.0 ± 2.6	38.5 ± 2.2	38.6 ± 2.5
S/V (capillary) (μm^{-1})	2.1 ± 0.1	1.9 ± 0.1	3.2 ± 1.4	1.5 ± 0.1	1.6 ± 0.1	2.4 ± 0.1	1.8 ± 0.1
S/V (lumen) (μm^{-1})	6.3 ± 1.1	10.2 ± 2.6*	6.5 ± 0.9	6.2 ± 0.9	5.6 ± 0.9	7.5 ± 0.7	6.2 ± 1.1
S_V (lumen, capillary) (%)	1.2 ± 0.1	1.4 ± 0.1	1.2 ± 0.1*	0.8 ± 0.1*	1.0 ± 0.1*	2.0 ± 0.1*	1.3 ± 0.1

Data are shown for the area of the capillary lumen, volume density (V_V) of the lumen compared to the capillary, surface area to volume ratio (*S/V*) of the capillary, *S/V* of the lumen, and surface density (S_V) of the lumen relative to the capillary area for control, L-NNA treated (L-NNA), extirpated (Ext), contralateral limb (CL), extirpated with L-NNA (E + L-NNA), prazosin treated (Praz) and prazosin with L-NNA (P + L-NNA). Mean ± S.E.M. $^*P < 0.05$ *versus* control.

Table 3. PCNA staining colocalizing with capillaries ($PCNA_{cap}$) and PCNA staining found in the interstitium ($PCNA_{int}$)

	$PCNA_{cap}$ (mm^{-2})	$PCNA_{int}$ (mm^{-2})
control	95 ± 30	30 ± 8
3d praz	75 ± 18	18 ± 5
7d praz	85 ± 15	24 ± 6
14d praz	96 ± 16	21 ± 5
3d ext	226 ± 34*	56 ± 8*
7d ext	157 ± 19*	35 ± 6
14d ext	167 ± 23*	33 ± 4
3d cl	103 ± 38	31 ± 19
7d cl	133 ± 30	39 ± 18
14d cl	141 ± 24	33 ± 7
3d ext + L-NNA	256 ± 34	71 ± 11
3d plaz + L-NNA	143 ± 31	25 ± 5

Mean ± S.E.M. $^*P < 0.05$ *versus* control.

allow analysis of molecular pathways, given current gene modulation technology and reagent availability. Angiogenesis in response to muscle extirpation or prazosin administration occurs to a comparable degree at 14 days. This appears to be an effective end-point as capillaries then appear structurally quiescent and not different from control (data not shown). Little further angiogenesis was seen between 14 and 28 days in either model in the mouse, whereas a modest increase in C:F was seen up to 8 weeks in the rat (Egginton *et al.* 1998). The angiogenesis seen in response to prazosin administration and extirpation in the mouse thus has a slightly different time course to angiogenesis seen in the rat, being largely completed earlier, with the rate peaking before 7 days in both models.

Seven days after prazosin administration, activation of ECs seen in this study represents an angiogenic pathway proceeding by longitudinal division of capillaries (Egginton *et al.* 2001). This can be achieved either by luminal filopodia extending across the lumen and fusing with opposing cytoplasm prior to capillary separation, or by extensive vacuolisation of a thickened endothelium, resulting in new capillaries. Seven days after extirpation, ECs are also activated but accompanied by an increase in cell number, proliferation index and capillary size, as well as a greater number of small abluminal sprouts associated with a focal disruption of the basement membrane. Previous studies have shown a conflicting response of pericytes during angiogenesis depending on the stimulus (Egginton *et al.* 2000). In this model, there appears to be a key role for both pericytes and fibroblasts in supporting angiogenesis, with both increasing in their capillary association, consistent with other skeletal muscle models (Egginton *et al.* 1996, 2001; Hansen-Smith *et al.* 2001). These characteristics show that abluminal sprouting through a weakened basement membrane is the major mechanism involved in forming new capillary anastomoses (Haas *et al.* 2000). Interactions with coagulation and inflammatory factors from surgery may occur, but these are likely to be of minor importance as sham-operated animals show a control phenotype. A novel observation was the high proportion of abluminal sprouts in physical contact with pericyte processes, suggesting a significant role for pericytes in directing these sprouts, consistent with *in vitro* data suggesting they may aid EC migration through modification of the extracellular matrix (Nehls *et al.* 1994). There was an increase in luminal filopodia (though to a much lesser extent than with prazosin administration) and level of vacuolisation, which suggests a minor common pathway with that seen in response to prazosin administration which is not evident in the rat. However, we do not believe this is due to increased shear stress as there is no measurable increase in blood flow. Whether this reflects allometric differences in basal shear stress

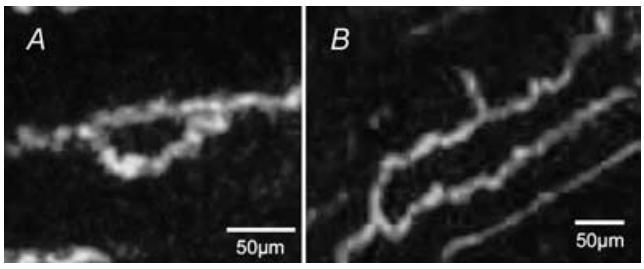

Figure 7. Morphological characterization of the angiogenic response
Extended focus (20 μm) images of a capillary loop in the prazosin model (*A*) and a capillary sprout in the extirpation model (*B*) are shown.

Table 4. Mitochondrial volume density

	Control	L-NNA	CL	Ext	E + L-NNA	Praz	P + L-NNA
Z1	26.6 ± 1.2	25.1 ± 1.2	24.4 ± 1.1	26.6 ± 1.5	27.67 ± 1.5	23.01 ± 1.4	23.35 ± 1.4
Z2	23.3 ± 3.8	21.1 ± 3.4	21.4 ± 1.1	26.1 ± 1.4	26.5 ± 1.2	19.9 ± 1.3	19.1 ± 1.1
Z3	16.4 ± 0.8	15.7 ± 0.9	17.5 ± 1.0	23.3 ± 1.2	21.3 ± 0.9	16.7 ± 1.1*	13.7 ± 0.7*
Total	21.2 ± 0.9	19.3 ± 0.8	20.7 ± 0.9	25.0 ± 1.0*	24.3 ± 0.9*	19.5 ± 1.1	18.3 ± 0.9

The mean mitochondrial V_V in a region approximating half the intercapillary distance is shown for control, L-NNA treated (L-NNA), extirpated (Ext), contralateral limb (CL), extirpated with L-NNA (E + L-NNA), prazosin treated (Praz) and prazosin with L-NNA (P + L-NNA). Z1, zone 1; Z2, zone 2; Z3, zone 3. Mean ± S.E.M. *$P < 0.05$ *versus* control.

accompanying differences in metabolism-coupled blood flow, or a transient change completed before observation is unclear. We propose that in the prazosin model, the predominant mechanical stimulus is increased shear stress acting from the vessel lumen. Although several genes have shear stress response elements, the transduction of altered shear stress to a genetic response remains unclear, but may involve an interplay between integrins and VEGF receptor 2 (VEGFR-2) (*Flk-1*) (Shyy, 2001; Wang *et al.* 2004). There may also be a role for shear-induced degradation of the glycocalyx via mechanical perturbation to expose the underlying endothelium (Brown *et al.* 1996). In the extirpation model, a number of factors acting from the abluminal surface of capillaries may influence angiogenesis, including activity of stretch-activated ion channels, or mechanical stretch of the cytoskeleton (Ingber, 2002). There is an increase in Matrix metalloprotease (MMP) levels during sprouting angiogenesis, but not in longitudinal splitting (Rivilis *et al.* 2002), which probably mediates the proteolytic breakdown of the basement membrane seen in our study. This could provide a route for the physical extension of activated EC. In addition, the basement membrane can act as a reservoir for growth factors, sequestering Basic fibroblast growth factor (FGF-2) and larger VEGF isoforms which may be released by mechanical perturbation or proteolysis (Folkman & Shing, 1992; Egginton *et al.* 2001).

Both forms of angiogenesis resulted in an increase in eNOS protein levels, although pharmacological inhibition of all NOS isoforms abolished the angiogenic response to prazosin, but not that in response to extirpation, suggesting that these two morphologically different mechanisms proceed via different molecular pathways. End-point analysis showed that $eNOS^{-/-}$ mice fail to respond to prazosin administration while $nNOS^{-/-}$ mice responded normally, as previously reported (Baum *et al.* 2004); however, both sets of mice responded to extirpation in a similar manner to wild-type mice. There was no increase in iNOS protein in either model, which suggests that NO generated from eNOS is required for shear-induced angiogenesis and that there is a separate, NO-independent pathway which is responsible for overload-induced angiogenesis. While it is possible that NO could be necessary for the arteriolar vasodilatation responsible for the increase in capillary shear stress, NO and PGI_2 have been shown to be equally responsible for basal tone and vasodilatation *in vivo* with compensatory cross-talk between the two (Hudlicka, 1991; Osanai *et al.* 2000). Administration of indomethacin causes only a partial inhibition of angiogenesis (Hussain & Egginton, 2005), so the complete abolition of angiogenesis seen in the present study is unlikely to be due to a reduction in the level of shear stress in our model.

NO appears to play an important role in the cellular angiogenic response to chronic shear stress, resulting in longitudinal division of the lumen, as the endothelial responses were all abolished by administration of L-NNA. The proliferative response of the endothelium in response to extirpation, abluminal EC responses and perivascular cell association may be characterized as part of an NO-independent pathway. It is interesting that those variables which were also seen in the shear response (i.e. luminal filopodia, vacuolization and cytoplasmic thickening) were all abolished by L-NNA administration. We suggest that this is due to an abolition of a minor angiogenic pathway seen in the extirpation model, shown by the small decrease in C:F. The lack of increased blood flow after extirpation suggests that this eNOS-dependent pathway can be stimulated by factors other than increased shear stress, and both stretch and shear have been shown to stimulate eNOS activity in endothelial cells *in vitro* (Fleming & Busse, 2003).

NO can have effects on cellular metabolism, especially respiration (Brown, 1995). Low levels of NO stimulate mitochondrial biogenesis (Gow & Stamler, 1998), whereas high levels can block mitochondrial respiration (Brown, 1995). This is consistent with the suggestion that the variable concentration of NO used in different experiments underlies the controversial role of NO in angiogenesis (Jones *et al.* 2004). In the current study, changes in mitochondrial content indicate that there is a tissue response to extirpation, probably due to increase in metabolic demand to support remodelling of the muscle (Goldspink, 1998) and sprouting angiogenesis. Little change in mean fibre area was seen in either model; the extirpation model showed an increase in

fibre size (hypertrophy) balanced by the generation of smaller fibres (hyperplasia) resulting in no net change. This is consistent with a combination of muscle stretch and overload (Kelley, 1996). The influence of NO on cellular metabolism appears to be negligible (Table 4) with neither an inhibitory (Brown, 1995) or up-regulatory (Gow & Stamler, 1998) influence on mitochondria in these two types of physiological angiogenesis. Therefore, NO probably affects angiogenesis directly rather than indirectly through metabolic effects.

In conclusion, we have shown that the two morphologically different forms of angiogenesis in skeletal muscle are mediated through different molecular pathways, one of which is dependent on NO. Inhibition of NO results in abolition of distinct parts of the angiogenic response to vasodilatation (luminal filopodia and vacuolisation), while leaving endothelial proliferation and capillary sprouting unaffected. These data show that NO mediates specific events during the longitudinal splitting of capillaries, but has no effect on classical capillary sprouting *in vivo*. This suggests that therapeutic angiogenesis mediated by NO donors does not occur via classical sprouting angiogenesis, and antiangiogenic therapies involving NO inhibition may have limited application.

References

Baum O, Da Silva-Azevedo L, Willerding G, Wockel A, Planitzer G, Gossrau R, Pries AR & Zakrzewicz A (2004). Endothelial NOS is main mediator for shear stress-dependent angiogenesis in skeletal muscle after prazosin administration. *Am J Physiol Heart Circ Physiol* **287**, H2300–H2308.

Brown GC (1995). Nitric oxide regulates mitochondrial respiration and cell functions by inhibiting cytochrome oxidase. *FEBS Lett* **369**, 136–139.

Brown MD, Egginton S, Hudlicka O & Zhou AL (1996). Appearance of the capillary endothelial glycocalyx in chronically stimulated rat skeletal muscles in relation to angiogenesis. *Exp Physiol* **81**, 1043–1046.

Egginton S, Hudlicka O, Brown MD, Graciotti L & Granata AL (1996). In vivo pericyte–endothelial cell interaction during angiogenesis in adult cardiac and skeletal muscle. *Microvasc Res* **51**, 213–228.

Egginton S, Hudlicka O, Brown MD, Walter H, Weiss JB & Bate A (1998). Capillary growth in relation to blood flow and performance in overloaded rat skeletal muscle. *J Appl Physiol* **85**, 2025–2032.

Egginton S, Hudlicka O & Glover M (1993). Fine structure of capillaries in ischaemic and non ischaemic rat striated muscle. Effect of torbafylline. *Int J Microcirc Clin Exp* **12**, 33–44.

Egginton S & Sidell BD (1989). Thermal acclimation induces adaptive changes in subcellular structure of fish skeletal muscle. *Am J Physiol* **256**, R1–R9.

Egginton S, Zhou AL, Brown MD & Hudlicka O (2000). The role of pericytes in controlling angiogenesis in vivo. *Adv Exp Med Biol* **476**, 81–99.

Egginton S, Zhou AL, Brown MD & Hudlicka O (2001). Unorthodox angiogenesis in skeletal muscle. *Cardiovasc Res* **49**, 634–646.

Fleming I & Busse R (2003). Molecular mechanisms involved in the regulation of the endothelial nitric oxide synthase. *Am J Physiol Regul Integr Comp Physiol* **284**, R1–R12.

Folkman J (1995). Angiogenesis in cancer, vascular, rheumatoid and other disease. *Nat Med* **1**, 27–31.

Folkman J & Shing Y (1992). Control of angiogenesis by heparin and other sulfated polysaccharides. *Adv Exp Med Biol* **313**, 355–364.

Fukumura D, Gohongi T, Kadambi A, Izumi Y, Ang J, Yun CO, Buerk DG, Huang PL & Jain RK (2001). Predominant role of endothelial nitric oxide synthase in vascular endothelial growth factor-induced angiogenesis and vascular permeability. *Proc Natl Acad Sci U S A* **98**, 2604–2609.

Goldspink G (1998). Cellular and molecular aspects of muscle growth, adaptation and ageing. *Gerodontology* **15**, 35–43.

Gow AJ & Stamler JS (1998). Reactions between nitric oxide and haemoglobin under physiological conditions. *Nature* **391**, 169–173.

Haas TL, Milkiewicz M, Davis SJ, Zhou AL, Egginton S, Brown MD, Madri JA & Hudlicka O (2000). Matrix metalloproteinase activity is required for activity-induced angiogenesis in rat skeletal muscle. *Am J Physiol Heart Circ Physiol* **279**, H1540–H1547.

Hansen-Smith F, Egginton S, Zhou AL & Hudlicka O (2001). Growth of arterioles precedes that of capillaries in stretch-induced angiogenesis in skeletal muscle. *Microvasc Res* **62**, 1–14.

Hudlicka O (1991). What makes blood vessels grow? *J Physiol* **444**, 1–24.

Hudlicka O, Brown M & Egginton S (1992). Angiogenesis in skeletal and cardiac muscle. *Physiol Rev* **72**, 369–417.

Hussain A & Egginton S (2005). Shear-induced angiogenesis is independent of vasodilator mechanism. *Microcirculation* (**in press**).

Ingber DE (2002). Mechanical signaling and the cellular response to extracellular matrix in angiogenesis and cardiovascular physiology. *Circ Res* **91**, 877–887.

Jones MK, Tsugawa K, Tarnawski AS & Baatar D (2004). Dual actions of nitric oxide on angiogenesis: possible roles of PKC, ERK, and AP-1. *Biochem Biophys Res Commun* **318**, 520–528.

Kelley G (1996). Mechanical overload and skeletal muscle fiber hyperplasia: a meta-analysis. *J Appl Physiol* **81**, 1584–1588.

Morbidelli L, Chang CH, Douglas JG, Granger HJ, Ledda F & Ziche M (1996). Nitric oxide mediates mitogenic effect of VEGF on coronary venular endothelium. *Am J Physiol* **270**, H411–H415.

Morley JE & Flood JF (1992). Competitive antagonism of nitric oxide synthetase causes weight loss in mice. *Life Sci* **51**, 1285–1289.

Nehls V, Schuchardt E & Drenckhahn D (1994). The effect of fibroblasts, vascular smooth muscle cells, and pericytes on sprout formation of endothelial cells in a fibrin gel angiogenesis system. *Microvasc Res* **48**, 349–363.

Neylon M & Marshall JM (1991). The role of adenosine in the respiratory and cardiovascular response to systemic hypoxia in the rat. *J Physiol* **440**, 529–545.

Osanai T, Fujita N, Fujiwara N, Nakano T, Takahashi K, Guan W & Okumura K (2000). Cross talk of shear-induced production of prostacyclin and nitric oxide in endothelial cells. *Am J Physiol Heart Circ Physiol* **278**, H233–H238.

Rivilis I, Milkiewicz M, Boyd P, Goldstein J, Brown MD, Egginton S, Hansen FM, Hudlicka O & Haas TL (2002). Differential involvement of MMP-2 and VEGF during muscle stretch- versus shear stress-induced angiogenesis. *Am J Physiol Heart Circ Physiol* **283**, H1430–H1438.

Rogers PA & Gargett CE (1998). Endometrial angiogenesis. *Angiogenesis* **2**, 287–294.

Shizukuda Y, Tang S, Yokota R & Ware JA (1999). Vascular endothelial growth factor-induced endothelial cell migration and proliferation depend on a nitric oxide-mediated decrease in protein kinase Cdelta activity. *Circ Res* **85**, 247–256.

Shyy JY (2001). Mechanotransduction in endothelial responses to shear stress: review of work in Dr. Chien's laboratory. *Biorheology* **38**, 109–117.

Wagner RC (1980). Endothelial cell embryology and growth. *Adv Microcirc* **9**, 45–75.

Wang Y, Chang J, Li YC, Li YS, Shyy JY & Chien S (2004). Shear stress and VEGF activate IKK via the Flk-1/Cbl/Akt signaling pathway. *Am J Physiol Heart Circ Physiol* **286**, H685–H692.

Zhou AL, Egginton S, Brown MD & Hudlicka O (1998). Capillary growth in overloaded, hypertrophic adult rat skeletal muscle: an ultrastructural study. *Anat Rec* **252**, 49–63.

Ziche M, Morbidelli L, Choudhuri R, Zhang HT, Donnini S, Granger HJ & Bicknell R (1997). Nitric oxide synthase lies downstream from vascular endothelial growth factor-induced but not basic fibroblast growth factor-induced angiogenesis. *J Clin Invest* **99**, 2625–2634.

Acknowledgements

This work was supported by the British Heart Foundation. The authors wish to thank Dr Oli Baum of the Freie Universität Berlin for his kind gift of $eNOS^{-/-}$ and $nNOS^{-/-}$ mice.